



**HAL**  
open science

## Single subject analyses reveal consistent recruitment of frontal operculum in performance monitoring

Céline Amiez, Magdalena G. Wutte, Isabelle Faillenot, Michael Petrides, Borís Burle, Emmanuel Procyk

► **To cite this version:**

Céline Amiez, Magdalena G. Wutte, Isabelle Faillenot, Michael Petrides, Borís Burle, et al.. Single subject analyses reveal consistent recruitment of frontal operculum in performance monitoring. *NeuroImage*, 2016, 133, pp.266-278. 10.1016/j.neuroimage.2016.03.003 . hal-01383991

**HAL Id: hal-01383991**

**<https://hal.science/hal-01383991v1>**

Submitted on 4 Oct 2022

**HAL** is a multi-disciplinary open access archive for the deposit and dissemination of scientific research documents, whether they are published or not. The documents may come from teaching and research institutions in France or abroad, or from public or private research centers.

L'archive ouverte pluridisciplinaire **HAL**, est destinée au dépôt et à la diffusion de documents scientifiques de niveau recherche, publiés ou non, émanant des établissements d'enseignement et de recherche français ou étrangers, des laboratoires publics ou privés.

## Accepted Manuscript

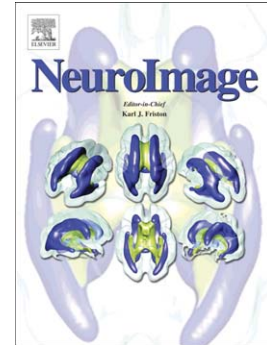
Single subject analyses reveal consistent recruitment of frontal operculum in performance monitoring

Céline Amiez, Magdalena G. Wutte, Isabelle Faillenot, Michael Petrides, Boris Burle, Emmanuel Procyk

PII: S1053-8119(16)00199-3  
DOI: doi: [10.1016/j.neuroimage.2016.03.003](https://doi.org/10.1016/j.neuroimage.2016.03.003)  
Reference: YNIMG 13006

To appear in: *NeuroImage*

Received date: 19 June 2015  
Accepted date: 2 March 2016



Please cite this article as: Amiez, Céline, Wutte, Magdalena G., Faillenot, Isabelle, Petrides, Michael, Burle, Boris, Procyk, Emmanuel, Single subject analyses reveal consistent recruitment of frontal operculum in performance monitoring, *NeuroImage* (2016), doi: [10.1016/j.neuroimage.2016.03.003](https://doi.org/10.1016/j.neuroimage.2016.03.003)

This is a PDF file of an unedited manuscript that has been accepted for publication. As a service to our customers we are providing this early version of the manuscript. The manuscript will undergo copyediting, typesetting, and review of the resulting proof before it is published in its final form. Please note that during the production process errors may be discovered which could affect the content, and all legal disclaimers that apply to the journal pertain.

## Single subject analyses reveal consistent recruitment of frontal operculum in performance monitoring

**Authors :** Céline Amiez<sup>1,2,\*</sup>, Magdalena G. Wutte<sup>3,\*</sup>, Isabelle Faillenot<sup>2,4,5</sup>, Michael Petrides<sup>6</sup>, Boris Burle<sup>3</sup>, Emmanuel Procyk<sup>1,2</sup>

**Affiliations :**

<sup>1</sup> Inserm U1208, Stem Cell and Brain Research Institute, 18 Avenue Doyen Lépine, 69500 Bron, France;

<sup>2</sup> Université de Lyon, Université Lyon 1, Lyon, France.

<sup>3</sup> Aix-Marseille Université, CNRS, LNC UMR 7291, 13331 Marseille, France

<sup>4</sup>Department of Neurology, Pain Center, CHU de Saint-Etienne, France.

<sup>5</sup>INSERM U879, UJM Saint-Etienne, France.

<sup>6</sup>Montreal Neurological Institute, McGill University, Montreal, Quebec H3A2B4, Canada.

\*The two first authors contributed equally to this work.

**Corresponding author:**

Céline Amiez, Ph.D.

INSERM U846, Stem Cell and Brain Research Institute

69675 Bron, France

Tel: +33 4 72 91 34 50, Fax: +33 4 72 91 34 61

Email: celine.amiez@inserm.fr

**Short title:** Performance monitoring and frontal operculum

**Keywords:** frontal operculum, anterior insula, feedback, fMRI, human

**Pages:** 33, **Figures:** 10, **Tables:** 1, **Supplemental tables:** 3

## Abstract

There are continuing uncertainties regarding whether performance monitoring recruits the anterior insula (al) and / or the frontal operculum (fO). The proximity and morphological complexity of these two regions make proper identification and isolation of the loci of activation extremely difficult. The use of group averaging methods in human neuroimaging might contribute to this problem. The result has been heterogeneous labelling of this region as al, fO, or al/fO, and a discussion of results oriented towards either cognitive or interoceptive functions depending on labelling. In the present article, we adapted the spatial preprocessing of functional magnetic resonance imaging data to account for group averaging artefacts and performed a subject by subject analysis in three performance monitoring tasks. Results show that functional activity related to feedback or action monitoring consistently follows local morphology in this region and demonstrate that the activity is located predominantly in the fO rather than in the al. From these results we propose that a full understanding of the respective role of al and fO would benefit from increased spatial resolution and subject by subject analysis.

## Introduction

Neuroimaging studies have shown that an extensive region located at the junction of the anterior insula (al) and the frontal operculum (fO) is an integral part of the performance monitoring network. The al and the fO are distinct cytoarchitectonic areas: whereas al is an agranular area, fO is a dysgranular area (Foundas et al., 2001; Anwander et al., 2007; Keller et al., 2009; Amunts et al., 2010; Keller et al., 2011; Nieuwenhuys, 2012). Differences in the presence and extent of granular layer IV have been shown to relate to differences in function. For instance, a striking difference is observed between primary sensory (granular) and primary motor (agranular) areas initially described by Brodmann. On a more fine-grained level, adjacent motor regions for example show different granularity (primary motor cortex agranular, premotor cortex dysgranular), for which a functional theory has been put forward (Shipp 2013). As such, the difference in granularity in al and fO would point towards distinct functional contributions of these areas to performance monitoring but which have been difficult to disentangle thus far.

The functional discrimination of these areas is difficult for different reasons: First, the morphological complexity of the region makes the proper identification of the locus of activation extremely challenging, especially using voxel-based neuroimaging methods. More precisely, whereas the circular insular sulcus (cris) delineating the insula is very stable across subjects, the intersection between al and fO displays morphological heterogeneity (Naidich et al., 2004; Nieuwenhuys, 2012). In addition, because of the local cortical folding, smoothed activation-related voxels may cover both fO and al subparts. Second, the fact that most studies use conventional linear group averaging methods amplifies this problem. As a result of these anatomical and technical challenges, authors label activity maxima in this region in various manners: they have been described as belonging to al (Preuschoff et al., 2008; Christopoulos et al., 2009; d'Acremont et al., 2009; Tobler et al., 2009; Rutledge et al., 2010; Ullsperger et al., 2010; Wessel et al., 2011; Amiez et al., 2012b; Harsay et al., 2012; Klein et al., 2013; Becker et al., 2014; Koban and Pourtois, 2014; Rothkirch et al., 2014), to fO (Higo et al., 2011; Nelissen et al., 2013), or to both (al/fO) (Menon et al., 2001; Dosenbach et al., 2006; Dosenbach et al., 2007; Fair et al., 2007; Seeley et

al., 2007; Sridharan et al., 2008; Amiez et al., 2012a; Vaden et al., 2013). Consequently, this imprecise labelling often leads to discussions of results orientated in the context of an al-related interoceptive/emotional perspective (e.g. Klein et al., 2007; Brass and Haggard, 2010; Ullsperger et al., 2010; Koban and Pourtois, 2014) or a cognitive perspective focussed on the fO (e.g. language) (e.g. Friederici et al., 2006; Higo et al., 2011). The specific aim of the present study was to assess whether these two regions can be dissociated with the spatial resolution of fMRI, and whether events related to performance monitoring recruit fO and/or al.

We took advantage of three studies originally designed to assess the function of the midcingulate cortex (MCC) in performance monitoring (Amiez et al. 2013; Wutte et al. in prep) and we resorted to subject by subject analysis to assess precise structure-to-function relationships. Such analysis consists in performing linear registration in MNI space of individual subject data and assess local relationship between sulcal morphology and functional activity in each hemisphere of each subject. This analysis has the advantage to keep intact the within subject relationships between sulci and gyri and that the MNI coordinates can be compared with other neuroimaging studies (and may be used for future meta-analyses). This analysis has already demonstrated its value for the understanding of the anatomo-functional organization of the primary hand motor cortex (Yousry et al. 1997), the dorsal premotor cortex (Amiez et al. 2006; Amiez and Petrides, 2009), the inferior frontal junction (Derrfuss et al., 2012), the mid-cingulate cortex (Amiez et al., 2013; Amiez and Petrides, 2014; Procyk et al. 2014), the angular gyrus (Segal and Petrides, 2013), the postcentral cortex (Zlatkina et al. 2015), and the dorsolateral prefrontal cortex (Amiez and Petrides, 2007) (for comments on this method, see Tomaiuolo and Giordano 2015). Note that such precise analysis may contribute to the improvement of future group-averaging methods based on non-linear/diffeomorphic brain registration targeted in this al/fO region, and therefore to allow a better spatial and statistical detection of activity increases (Auzias et al 2011; Pizzagalli et al 2013).

Previous work shows systematic co-activation of MCC and al/fO during performance monitoring (Dosenbach et al., 2006; Dosenbach et al., 2007; Higo et al., 2011; Amiez et al., 2012a; Amiez et al., 2012b; Amiez et al., 2013), both after relevant feedbacks (Amiez et al., 2012a; Amiez et al., 2012b; Amiez et al., 2013), and action

errors (Klein et al., 2007, Ullsperger & von Cramon, 2004, Wessel et al., 2012). We here focus on this co-activated al/fO region and perform subject by subject analyses in order to assess the relationships between local al and fO morphology and activation related to performance monitoring.

Classical cytoarchitectonic studies have delineated the opercular cortical region that lies next to the pars opercularis (BA 44) and pars triangularis (BA 45) (see Petrides 2014 for discussion). For instance, Economo and Koskinas refer to the opercular region adjacent to the pars opercularis as area FCDop and the opercular region adjacent to the pars triangularis as area FDop (Economo and Koskinas, 1925) and Petrides (2014) as areas 44op and 45op. A recent receptor architectonic study (Amunts et al., 2010) demonstrated the existence of four fO areas: Op8, located adjacent to area 44; Op9, located adjacent and ventral to area 45; Op7, located adjacent to Op8, and Op10, located adjacent to Op9 (Fig. 1). These fO areas display different receptor types distributions than those observed in area 44 and 45. Taking differences in granularity and receptor organization together, we can hypothesize important functional dissociations between al, fO areas (Op7, 8, 9, 10), and lateral frontal areas 44/45, as other authors suggested (Nieuwenhuys, 2012; Morel et al., 2013; Neubert et al., 2014). This anatomo-functional organization is also supported by a diffusion-weighted magnetic resonance imaging study showing a segregation of areas 44, 45, and fO on the basis of differential connectivity (Anwander et al., 2007).

-----Figure 1 about here-----

The current study aimed therefore to locate the activations observed at the intersection of the circular insular sulcus and frontal operculum with reference to the organization of the cytoarchitectonic areas described above. The results demonstrated that performance monitoring activity is mainly associated to the fO and not (or very weakly to) the al. We provide precise methodological steps to help further studies in the identification of the locus of activations in the al/fO region.

## Materials and Methods

The methods related to study 1 have been published previously (Amiez et al., 2013) and will therefore be presented briefly here. The methods of studies 2 and 3 have not been published and will be presented in greater detail.

Study 1 and 2 relate to feedback monitoring during trial and error learning with respectively juice feedback and visual feedback. Study 3 corresponds to a compatibility task challenging action monitoring and error processing referred to as 'internal' feedback processing.

These studies were performed in accordance with the Declaration of Helsinki and approved by the local ethics committees. All participants gave written consent to participate in these studies. All of them had normal or corrected-to-normal vision. None of them was taking medication or had any history of neurological disease.

### ***Participants***

**Studies 1 and 2.** Fifteen right-handed healthy volunteers (7 female, mean age = 26.3), participated in the first fMRI study. Twelve of them (6 female) participated in the second study.

**Study 3.** Thirty-two healthy volunteers participated in this study. Two subjects were excluded from the MR analysis due to neurological findings resulting in a final cohort of 30 subjects (10 female, mean age = 23). Handedness was assessed with the 'Handedness Inventory' (Oldfield, 1971). All but one subject were right handed, with handedness scores from 33-100 (+100 fully right handed, -100 fully left-handed).

### ***Protocol***

#### **Studies 1 and 2**

In these two studies, subjects performed a problem-solving task in which they had to discover by trial and error in successive trials which one of three simultaneously presented abstract stimuli was associated with positive feedback. In each successive "problem", subjects searched for and then exploited the correct response. Hence, two periods were distinguished in this task: an exploration period in which negative feedback (instructing change in the stimulus choice, called "NEGexplore") and the first

positive feedback (instructing the subject to stop exploring and to start exploiting, called “POSexplore”) were received, and an exploitation period in which the subject repeated the correct choice and in which positive feedback was received (called “POSexploit”). In each trial, three abstract unknown stimuli appeared simultaneously at the three possible locations on the screen for 2s. During these 2s, the subjects had to select one of these stimuli by pressing the corresponding mouse button. Note that the spatial position of each stimulus varied randomly from trial to trial throughout a problem, thus rendering the spatial information irrelevant to task performance. After a delay varying from 0.5 to 6s (average = 2s), a feedback was delivered. If the choice was incorrect, a negative feedback stimulus was presented and, after an inter-trial interval pseudo-randomly varying from 0.5 to 8s (average = 3.5s), the same 3 stimuli were presented again at different spatial positions and the subject would make another selection. Testing proceeded in this manner until the subject found the correct stimulus, the correct choice being indicated by the delivery of the positive feedback. After the first correct choice (associated with the delivery of the first positive feedback), the exploration period terminated and the exploitation period started. The exploration period lasted 1–3 trials and the exploitation period consisted of 2 trials during which the subject could keep selecting the correct stimulus. When a problem was solved, three new novel abstract stimuli were presented and the subject attempted to solve the new problem.

-----Figure 2 about here-----

In study 1 (**Fig 2A**), various volumes of fruit juice were used to provide the feedback. To equalize as much as possible sensory information provided for negative versus positive feedback, we designed 4 conditions in which negative feedback could be juice delivery. In every condition, the positive feedback corresponded to the largest reward delivery. In conditions 1, 2, 3, and 4, the positive and negative feedback values were 1.2 and 0 ml, 1.2 and 0.4 ml, 0.8 and 0 ml, and 0.8 and 0.4 ml of fruit juice, respectively. These four conditions were pseudorandomly selected for each problem. The subject was informed of the condition type by the color of the fixation cross presented in the center of the screen (see Fig 1A). To control for motivational state, subjects were asked not to drink for 12 h before the experiment. Note that behavioural data have been published in Amiez et al. (2013).

In study 2 (**Fig 2B**), negative feedback was a red square, positive feedback was a green square. These two types of feedback were presented during 1s.

Problems were labelled as correct when no repetition of incorrect choices occurred in the exploration period and no incorrect choices occurred in the exploitation period. Only data obtained from problems solved correctly were used for fMRI analysis.

### **Study 3**

Participants conducted an audio-visual accessory Simon task, during which they had to respond with a left or a right button-press to the color of a centrally presented stimulus (**Fig 2C**). Participants were instructed to respond as fast as possible. The stimulus color was either red or green. Concurrently, a distractor sound was played to the left or the right ear. The side of response and the sound were either on the same (compatible) or on opposite sites (incompatible). This caused a compatibility effect as observed in longer reaction times and higher error rates on incompatible trials. Color-side of response instructions were counterbalanced across subjects.

396 trials were presented in three runs of 132 trials each. The same number of compatible and incompatible trials was presented. Randomizations were controlled to allow for not more than 3 repetitions per feature (side of response, color or compatibility).

The protocol consisted of a fast event-related design with events of 1.4 s durations. Events included a preparation time of 0.4 s and a stimulus duration of 1s for the visual and 100ms for the auditory stimulus. The inter-stimulus-interval (ISI) was jittered between 2.4 and 8.8 s (exponential distribution).

Trials on which participants did respond with the opposite hand than the one instructed to, are considered as errors and are at the core of this analysis. These erroneous responses are well known to recruit the action monitoring network (Ridderinkhof et al., 2004). Trials following errors showed post-error slowing (mean reaction times pre-error-trials: 374 ms, error trials: 344 ms, post-error trials: 398 ms, pre-error trials are faster than post-error trials,  $p < 0.001$ ) Previous studies have shown that post-error slowing can be in great parts be attributed to an increase in response caution (Rabbitt, 1966; Ridderinkhof et al., 2004; Dutilh et al., 2011). We therefore

assumed that errors served as internal feedback to refocus action monitoring. Missed trials were excluded. All other trials are modeled as correct trials. Note that no external feedback was provided.

### ***MRI acquisition***

**Studies 1 and 2.** Each volunteer was scanned using a 1.5T Siemens Sonata MRI Scanner (Siemens). Brain imaging acquisitions were performed at the imaging facility (*CERMEP-imagerie du vivant, Bron, France*). After a high-resolution T1 anatomical scan (whole head, 1mm<sup>3</sup> isotropic resolution, TR=1.97s, TE=0.393s, flip angle=15°), five functional runs of 260 images each (37 oblique T2\* gradient echoplanar images, voxel size 3.4x3.4x3.4 mm, TR=3.5 s, TE=50 ms, flip angle=90°) sensitive to the blood oxygenation level-dependent (BOLD) signal were acquired. The field of view covered the whole brain. The first trial onset in each run was synchronized with the scanner acquisition via a trigger signal generated by the scanner. Behavioral and imaging data were acquired in all trials.

**Study 3.** Imaging data was acquired on a 3-T Bruker Medspec 30/80 Advance whole body MRI system, equipped with a circular polarized head coil using Echo-planar imaging (EPI) (TR: 2.4 s, echo time: 30 ms, flip angle: 81.6°). Brain imaging acquisitions were performed at the Marseille fMRI center (*Marseille, France*). 36 slice volumes were acquired (interleaved acquisition) with a voxel size of 3 x 3 x 3 mm. Three functional runs of 191 volumes each were acquired. Before the functional runs, a high-order shim was performed and a fieldmap was scanned. Additionally, a T1- weighted anatomical volume was acquired (whole head, 1mm<sup>3</sup> isotropic resolution, TR=0.94s, TE=0.4424s, flip angle = 90°). For the purpose of another study, an additional functional run (auditory localizer, 141 volumes) and a diffusion-tensor imaging sequence were scanned in the same participants.

### ***Data analysis***

**fMRI data: Studies 1 and 2**

Preprocessing and data analysis were performed with Statistical Parametric Mapping software (SPM12b; Wellcome Department of Cognitive Neurology, University of College London, London, UK; <http://www.fil.ion.ucl.ac.uk/spm>) and Matlab 8.2 ([www.mathworks.com](http://www.mathworks.com)). In order to precisely assess the location of increased activity in al/fO, preprocessing was optimized. The first five volumes of each run were removed to allow for T1 equilibrium effects. We applied a head motion correction using rigid-body realignment and an unwarped algorithm allowing to reduce spatial EPI distortion. Then, slice-timing correction was applied using the time center of the volume as reference. The Artifact detection Toolbox (ART, [http://www.nitrc.org/projects/artifact\\_detect/](http://www.nitrc.org/projects/artifact_detect/)) was used to remove outliers, i.e. volumes in which movement parameters were superior to 2 SD from the mean. The subject-mean functional MR images were then co-registered with the corresponding structural MR images using mutual information optimization. Functional images were spatially normalized into standard MNI space at the EPI resolution, i.e. 3.4mm<sup>3</sup>. Finally, functional images were smoothed using the EPI resolution 3.4mm fullwidth half-maximum Gaussian kernel for the individual subject analysis and using the EPI resolution 6mm fullwidth half-maximum Gaussian kernel for the group analysis (Friston et al., 1995b; Friston et al., 1995a; Friston et al., 1995c). A 128s temporal high-pass filter regressor set was included in the design matrix to exclude low-frequency confounds.

At the first level, each trial was modelled with impulse regressors at the time of the presentation of the different types of feedback. These regressors were then convolved with the canonical hemodynamic response function and entered into a general linear model (GLM) of each subject's fMRI data. The six scan-to-scan motion parameters produced during realignment and outliers were included as additional regressors in the general linear model to account for residual effects of subject movement. At the second level, we first generated single-subject contrast images and compiled the corresponding group (from 15 and 12 subjects in studies 1 and 2, respectively) contrast images. For both the group and individual subject levels, we performed whole-brain analyses. Increased activity at the occurrence of feedback during the exploration period was assessed by comparing the Blood Oxygen Level Dependent (BOLD) signal at the occurrence of negative feedback during exploration

with the positive feedback during exploitation (i.e. NEGexplore minus POSexploit), and by comparing the BOLD signal at the occurrence of the first positive feedback (exploration) with positive feedback in exploitation (i.e. POSexplore minus POSexploit). In the group analysis (see **Figs. 3-4**), we then performed a spatial conjunction (Friston et al., 2005), between these two comparisons. Specifically, the conjunction analysis was implemented using the minimum of the t statistic obtained from “NEGexplore minus POSexploit” and “POSexplore minus POSexploit” contrasts in the group analysis of studies 1 and 2 (Friston et al. 2005). Thus, only those voxels from each contrast that survived a common threshold were considered significantly activated in the conjunction analysis. Significance was assessed on the basis of the spatial extent of consecutive voxels. A cluster volume extent  $>190 \text{ mm}^3$  in study 1 and  $>195 \text{ mm}^3$  in study 2 with a t-value  $>3$  was significant ( $P<0.05$ ), corrected for multiple comparisons using the method of Friston et al. (1995).

Because the group analysis revealed that the same brain regions showed increased activity in “NEGexplore minus POSexploit” and “POSexplore minus POSexploit” in both studies 1 and 2 (see result section), we combined negative feedback and first positive feedback of exploration and contrasted it with positive feedback in exploitation (i.e. [NEGexplore + POSexplore] – POSexploit) in the individual subject analysis (see **Fig. 6-8**). The resulting single-subject contrast images were used in the following group analyses and results are presented at  $p<0.001$  uncorrected. At the second level, we compiled the corresponding group (from 15 and 12 subjects in studies 1 and 2, respectively) contrast images. The resulting t statistic images were thresholded using the minimum given by a Bonferroni correction and random field theory to account for multiple comparisons (FWE). Group level results are presented both at  $p<0.05$  FWE and at  $p<0.001$  uncorrected.

Note that, in study 1, the group analysis comprised 3343 exploration trials (i.e. 1825 negative and 1518 first positive feedback) and 2924 exploitative trials. The subject by subject analysis comprised, on average per subject, 223 exploration trials (i.e. 122 incorrect feedback + 101 first correct feedback) and 195 exploitative trials. In study 2, the group analysis comprised 1394 exploration trials (i.e. 702 negative and 692 first positive feedback) and 1382 exploitative trials. The subject by subject analysis

included, on average per subject, 116 exploration trials (i.e. 59 incorrect feedback + 58 first correct feedback) and 115 exploitation trials.

### **fMRI data: Study 3**

Data analysis was performed as described for studies 1 and 2, with the following alterations: Deformations of the magnetic field were estimated from the fieldmap and were used for unwarping. As functional images were acquired with a resolution of 3mm, they were smoothed at 3mm for individual analysis. For group analysis, data were smoothed at 6mm.

At the first-level, error and correct trials were modeled with impulse regressors at the time of stimulus presentation. GLM analysis on first and second level was performed as described above. To assess the BOLD signal specific to error processing, i.e. internal feedback, error trials were contrasted with correct trials (contrast "Error-Correct"). Note that there are considerably less error trials than correct trials (error-rate: 5.6 % on average, therefore 22 error trials vs 374 correct trials on average per subject). Statistical thresholding was carried out as described above.

### **Comparison between studies**

To assess the extent of the region commonly involved in the analysis of exploratory visual and juice external feedback and internal feedback, we also performed, at the group level, a spatial conjunction between the contrast "[NEGexplore + POSexplore] – POSexploit" in study 1, the contrast "[NEGexplore + POSexplore] – POSexploit" in study 2 and the contrast "Error-Correct" in study 3 (Friston et al., 2005). A cluster volume extent  $>179 \text{ mm}^3$  with a t-value  $>3$  was significant ( $P<0.05$ ), corrected for multiple comparisons using the method of Friston et al. (1995).

### **Anatomical criteria for subject by subject analysis:**

To define whether increased activity was located in Op8 or in Op9 in each subject, we first delineated areas 44 and 45, which occupy respectively the pars opercularis and the pars triangularis of the inferior frontal gyrus (Petrides and Pandya, 1994; Amunts et al., 1999; Petrides and Pandya, 2002; Amunts et al., 2010; Petrides, 2014). To assess

the antero-posterior extent of area 44, we therefore defined the inferior precentral sulcus (iprs) and the ascending anterior ramus of the lateral fissure (aalf), which correspond to the caudal and rostral limits of the pars opercularis (see Fig 2). To assess the antero-posterior extent of area 45, we identified the ascending anterior ramus of the lateral fissure (aalf) and the horizontal anterior ramus of the lateral fissure (half), which correspond to the caudal and rostral limits of the pars triangularis (Fig 1). Following the tradition in functional neuroimaging studies, the region located at the most anterior region of what seems a continuation of the insula was labelled as al. Note, however, that the insular cortex correlates with the claustrum and at this most anterior region, the claustrum is no longer present and the cortex here is cytoarchitectonically not a part of the insular cortex (see Nieuwenhuis 2012 for a discussion on Insula/claustrum relationships).

We then followed the operculum at the anteroposterior level of these regions up to the cris to define whether increased activity located in the operculum was in Op8 (44op) (if at the anteroposterior level of area 44) or in Op9 (45op) (if at the anteroposterior level of area 45). If increased activity was located at the intersection between Op8 and cris we labelled this region Op8/cris. If increased activity was located at the intersection between Op9 and cris, then we labelled this region Op9/cris (see Fig 1).

#### **Cluster analysis in individual subjects: overlap method.**

In order to assess the extent of the al/fO region involved in the analysis of external juice (study 1), external visual (study 2), and internal (study 3) feedback, we employed the method used to identify maps of lesion coverage in groups of patients with brain lesions (Damasio and Frank, 1992). This method provides precise information about the overall extent of lesions in a group of patients but also about the number of patients contributing to each voxel of the lesion map. To this end, clusters of activation were extracted in individual subjects at a threshold of  $p < 0.001$  uncorrected. Then, clusters from all subjects were summed (with the ImCalc SPM tool). The resulting maps show a color-coded gradient of the extent of regions commonly involved in  $n$

subjects (i.e. in red, activation zone common to the 15, 12, and 30 subjects in studies 1, 2, and 3, respectively, and in purple, zones activated only in 1 subject).

## Results

### Group analysis

#### *STUDY 1:*

Group results with a commonly used 6mm smoothing revealed bilateral increased activity related to the analysis of feedback during exploration (i.e. contrast [NEGexplore + POSexplore] – POSexploit) localized at the intersection between the *cris* and the *fO* (left hemisphere: MNI coordinates (x, y, z) -30, 20, 8, t-statistic = 10.12; right hemisphere: MNI coordinates (x, y, z) 30, 20, 4, t-statistic = 11.15), spreading both into *al* and *fO* (**Fig 3A**), preventing us from determining the precise location of this region. Note also that a group analysis with a smaller smoothing kernel (i.e. 3.4mm) did not allow us to precisely identify which region was concerned (see Tables S1 and Fig S1-top panel).

-----Figure 3 about here-----

We then compared all feedback in exploration (i.e. negative and first positive feedback – called NEGexplore and POSexplore) to positive feedback during exploitation (called POSexploit) because the two contrasts “NEGexplore minus POSexploit” and “POSexplore minus POS exploit” revealed increased activity at the exact same location at the intersection between *al* and *fO* (**Figs 3B, 3C**), as demonstrated by the group conjunction analysis (**Fig 3D**). Specifically, this analysis revealed increased activity at the intersection *fO/al* at MNI coordinates 34, 21, 8,  $t=6.74$  (voxel extent at  $t>3 = 1808\text{mm}^3$ ) in the right hemisphere and -30, 24, 2,  $t=4.31$  (voxel extent at  $t>3 = 865\text{mm}^3$ ) in the left hemisphere. We therefore focused on the contrast [NEGexplore + POSexplore] minus POSexploit.

Although it was not the focus of the study, we verified the specificity of *fO/al* activation regarding positive, negative feedback, and the amount of juice reward as in Amiez et al. (2013). The data revealed that the functional signature related to

feedback analysis in exploration/exploitation behaviors is similar in al/fO and in MCC (Amiez et al. 2013), i.e. at the level of our analyses, activations do not discriminate reward size nor feedback valence (data not shown).

### STUDY 2:

Given that a gustatory area has been described in the human frontal operculum (Small et al., 1999; Veldhuizen et al., 2011) and given that the feedback used in study 1 was juice reward, we conducted a second study in 12 subjects out of the 15 who participated in study 1, in which feedback was visual.

Group results with a usual 6mm smoothing demonstrated a bilaterally increased activity focus at the intersection of the *cris* and the fO (left hemisphere: MNI coordinates (x, y, z) -30, 20, 8, t-statistic = 6.13; right hemisphere: MNI coordinates (x, y, z) 34, 22, 8, t-statistic = 9.07). The activation spread both into al and fO (**Fig 4A**). Note also that a group analysis with a smaller smoothing kernel (i.e. 3.4mm) did not allow us to precisely identify the region (see Tables S2 and Fig S1-middle panel).

-----Figure 4 about here-----

As in study 1, we compared all feedback in exploration to positive feedback in exploitation (i.e. contrast [NEGexplore + POSexplore] minus POSexploit) because the two contrasts “NEGexplore minus POSexploit” and “POSexplore minus POS exploit” revealed increased activity at the exact same location at the intersection between al and fO (Figs 4B, 4C), as demonstrated by the group conjunction analysis (Fig 4D). Specifically, this analysis revealed increased activity at the intersection fO/al at MNI coordinates (x, y, z) 30, 20, 4,  $t=6.96$  (voxel extent at  $t>3 = 1965\text{mm}^3$ ) in the right hemisphere and -30, 20, 8,  $t=7.42$  (voxel extent at  $t>3 = 2240\text{mm}^3$ ) in the left hemisphere.

### STUDY 3

Group results revealed bilateral activation at the intersection of the *cris* and the fO, spreading both into al and fO (left hemisphere: MNI coordinates (x, y, z) -39, 11, -1, t-statistic = 7.77; right hemisphere: MNI coordinates (x, y, z) 30, 20, 4, t-statistic = 11.15). Finally, again, a group analysis with a smaller smoothing kernel (i.e. 3mm) did not allow us to precisely identify the region (see Tables S3 and Fig S1-bottom panel). The

increased activity was found at the same location as in studies 1 and 2 (**Fig 5**). The group analysis, thus, did not clarify whether the cluster of activation was located in fO or in al.

-----Figure 5 about here-----

#### **COMPARISON BETWEEN THE THREE STUDIES:**

In order to assess whether the fO/al region involved in the analysis of external and internal feedback is the exact same region, we performed a conjunction between the contrasts [NEGexplore + POSexplore] minus POSexploit) in studies 1 and 2 and "Error-Correct" in study 3. Data revealed a commonly located increased activity at the intersection between al and fO (right hemisphere: MNI coordinates (x, y, z) 34, 22, 8,  $t=6.18$  (voxel extent at  $t>3 = 2283\text{mm}^3$ ); left hemisphere: -30, 20, 8,  $t=5.32$  (voxel extent at  $t>3 = 1649\text{mm}^3$ )) (**Fig 6**). This reveals that external visual and juice feedback and internal error feedback induce activation in the same fO/al region.

-----Figure 6 about here-----

#### **Subject-by-subject analyses**

##### **STUDY 1**

We then performed a subject by subject analysis. Results of a typical subject are presented in **Fig 7A**. As it can be appreciated on horizontal slices, two foci (maxima of BOLD signal) of external juice feedback-related activity are observed: one within the frontal operculum Op9 area, and one at the intersection between Op9 and cris.

-----Figure 7 about here-----

Maxima of activity observed in all subjects are described in **Figs 8A and 9A**, and in Supplemental tables S1.

-----Figures 8 and 9 here-----

Results demonstrated that all subjects displayed, at least in one hemisphere, increased activity at the intersection between Op9 and *cris* (white circles, **Fig 9A**). A second maxima of activity was located within Op9 in 13 out of 15 subjects at least in one hemisphere (red circles, **Fig 9A**). Only 3 out of 15 subjects (in the left hemisphere of S10 and S11, and in the right hemisphere of S6, S10, and S11) displayed a maxima of activity within Op8 (pink circles, **Fig 9A**).

In order to assess the extent of the al/fO cluster involved in the analysis of external juice feedback during exploration, we employed the overlap method (see Method section). The resulting map (**Fig 10A**) shows a color-coded gradient of the extent of regions commonly involved in  $n$  subjects (i.e. in red, activation zone common to the 15 subjects, and in purple, zones activated only in 1 subject). The resulting region extended from the intersection of the *cris* and the fO to Op8/9 (see **Fig 10A**). This activity zone never spread into al.

-----Figure 10 here-----

Neubert et al. (2014) recently subdivided the ventrolateral prefrontal cortex, including fO, in 12 subregions on the basis of their tractography pattern. This parcellation shows that areas 44v and 45 extend into the frontal operculum (**Fig 10D**). We superimposed these 12 subregions (with permission to use Supplemental Material “Neuroimaging S2”, Neubert et al. 2014) onto our anatomical average horizontal sections of interest (at MNI Z coordinates 9, 6, 3, 0, -3, -6, and -9). Results are displayed in **Fig 10D** and suggest that the region involved in performance monitoring covers Op and also parts of 44v and 45.

## STUDY 2

As in study 1, the subject by subject results (**Figs 7B, 8B, 9B**) demonstrated two maxima of activity: one systematically located at the intersection between Op9 and *cris* (in 12/12 subjects in both hemispheres, white circles, **Fig 9B**) and one located within Op9 (in 11/12 subjects at least in one hemisphere, red circles, circles, **Fig 9B**). Some clusters were also located in Op8 (in 5 of 12 subjects at least in one hemisphere, pink circles, **Fig 9B**). Note that MNI coordinates of maxima of activity observed in all subjects are described in **Figs 8B and 9B**, and in **Supplemental table S2**.

We further assessed the extent of the al/fO cluster involved in the analysis of external visual feedback during exploration by employing the overlap methods (see above). The resulting region extended from the intersection of the *cris* and the fO to Op8/9 (see **Fig 10B**). According to Neubert et al.’s map (2014), the region involved would also cover parts of area 44v, 45 within fO (**Fig 10D**). Again, this activity increase was never located within al per se.

**STUDY 3:**

The subject by subject analysis (**Fig 7C, 8C, 9C**) demonstrated two clusters: one at the intersection of the *cris* and the *fO* (white circles, **Fig 9C**), the other in *Op9* (red circles, **Fig 5C**). Some clusters were also located in *Op8* (in 11 of 30 subjects, pink circles, **Fig 5C**). Note that in two subjects (out of 30) one of the clusters was located in *al* (*S10*, *S18*, see yellow circles in **Fig 9C**, and coordinates in figure **8C**). MNI coordinates of maxima of activity observed in all subjects are described in **Figs 8C, 9C**, and in Supplemental table S3.

We assessed the extent of the *al/fO* cluster involved in the analysis of internal feedback by employing the overlap method. Results are presented in **Fig 10C** and show that the region involved would also cover parts of area 44v, 45 within *fO*, according to Neubert et al. (2014) (**Fig 10D**).

**COMPARISON BETWEEN THE THREE STUDIES:**

As shown in Figs 8 and 9, Table 1, and Tables S1, S2, and S3, activity maxima are found in a large majority of cases at the intersection between *fO* and *cris* or within *Op8* or *Op9*. Importantly, the clusters extend predominantly in *fO*, as displayed in **Fig 10**.

**Discussion**

Feedback and error processing recruit a common network, including MCC and a lateral frontal region either termed *al*, *fO* or *al/fO* in the literature. Both summary analyses of activity maxima locations (**Fig 9**) and cluster extent in individual subjects (**Fig 10**) demonstrated that external feedback as well as error responses induce activation of cortex located at the intersection of the *cris* and the *fO*, spreading into *fO*. This region should correspond to *Op10* and *Op8/Op9* areas as described by Amunts and colleagues (2010) and covers the classical frontal operculum found along the inferior frontal gyrus, i.e. the opercular region next to the classical Broca region (Neubert et al., 2014). As such, we can reasonably conclude that the cortex involved in the analysis of internal (action error) and external feedback is not focussed on the anterior insular cortex (*al*) per se, but rather in the ventrolateral opercular region (*fO*).

It should be noted here that the insular cortex is anatomically related to the extent of the claustrum. At the most anterior part of the opercular cortex, at the level of area 45 (pars triangularis), the cortex that is often labelled as insula and appears a continuation of the anterior insula is not insular cortex (Petrides and Pandya, 1994). Thus, it is unlikely that activations so far anterior (i.e. at the level of area 45) would be insular activations. In any case, the present study shows that the activation does not even fall primarily within the region often labelled as al, at this most anterior part of the opercular region.

Our results have at least two implications. First, the anatomical location of fMRI local maxima falling in the region covering fO and al should be discussed with particular care. As demonstrated, it is almost impossible to attribute functional activity to either fO or al if one uses conventional linear group averaging methods, using either a large or a small smoothing kernel (Fig S1). Performance monitoring has been previously described as recruiting this broad region although in many studies it was referred to as either al (Preuschoff et al., 2008; Christopoulos et al., 2009; d'Acremont et al., 2009; Tobler et al., 2009; Rutledge et al., 2010; Ullsperger et al., 2010; Wessel et al., 2011; Amiez et al., 2012b; Harsay et al., 2012; Klein et al., 2013; Becker et al., 2014; Koban and Pourtois, 2014; Rothkirch et al., 2014), fO (Higo et al., 2011; Nelissen et al., 2013), or al/fO (Dosenbach et al., 2006; Higo et al., 2011). This approach creates major confusion not only concerning the respective implication/non-implication of the al and fO in performance monitoring, but also in the functional interpretation of action monitoring, since labelling this region as al or fO leads to very different discussion of results, either in terms of interoceptive/emotional (e.g. Klein et al., 2007; Brass and Haggard, 2010; Ullsperger et al., 2010; Koban and Pourtois, 2014) or cognitive perspective focussed on the fO (e.g. Friederici et al., 2006; Higo et al., 2011). The present studies show that performance monitoring recruits fO. Further experiments using optimized spatial preprocessing and precise analysis of relationships between sulcus morphology and functional activity at the individual subject level should allow a better understanding of the respective role of al and fO.

As shown in the present paper, linear group averaging methods do not allow to disambiguate the respective involvement of al and fO and constitute therefore a limitation to the group analysis in the present study. However, precise sulcal

morphological analysis could help the implementation of local diffeomorphic methods allowing to perform optimized non-linear group averaging analysis. Indeed, such method allows to independently normalize EPI data of a group of subjects according to local morphology (sulci patterns) in a given brain region (Auzias et al 2011; Pizzagalli et al 2013), and therefore to improve both the spatial localization of activation clusters and their statistical power.

Detailed comparisons of the anatomical organization of the al/fO region in the human with that of the monkey would certainly help understanding the functional dissociations observed in al versus in fO in the human brain (Petrides and Pandya, 1994). Future studies should establish anatomical correspondences of the sub-regions of al and fO between human and monkey. Based on the available literature, we might describe one converging point between the two species: the circular insular sulcus in the human and the corresponding limiting sulcus in the monkey might not be a landmark separating al from fO. Rather, at the intersection of the circular/limiting sulcus and the frontal operculum, there is an area called ldfa in monkey (see Evrard et al. 2014). In human, Amunts et al. (2010) describe an area called Op10, located medially to Op9. Whether this area extend within and beyond the circular/limiting sulcus, and whether this area and the monkey ldfa area are homologous are open questions.

The fO/al region is consistently co-activated with the mid-cingulate cortex (MCC), a key region for monitoring external and internal behavioural feedback (Holroyd et al., 2004; Rushworth et al., 2007a; Rushworth et al., 2007b; Rushworth et al., 2011; Amiez et al., 2012a; Amiez et al., 2012b; Amiez et al., 2013). In the MCC, as in fO, we observed increased activity in relation to the analysis of both gustatory (Amiez et al., 2012) and visual feedback during exploration (Amiez et al. in preparation). Both structures display similar functional signatures during our trial-and-error task and thus the present data do not allow to disentangle the respective role of MCC and fO in performance monitoring. It is interesting to note that these two regions share a similar cytoarchitectonic dysgranular organization. They might also both contain spiral-shaped neurons in the fifth layer, the so-called “von Economo neurons” (VENs) (von Economo and Koskinas, 1925; Allman et al., 2011; Nieuwenhuys, 2012). However, as for brain imaging data, the precise location and relative distributions of

VENs in the fO/al region are unclear. Precise anatomical accounts have shown the presence of VENs in the al (Morel et al. 2013). Other descriptions of the putative presence of VENs in fO are often insufficiently documented although they mention the presence of VENs in the transition cortex between al and fO (area FI of Economo and Koskinas) (Nimchinsky et al., 1999; Seeley et al., 2012; Nieuwenhuys, 2012). Thus whether VENs are present in the pure fO, and whether they reflect a specific functional cognitive network including MCC, fO and/or al, remains to be elucidated.

To conclude, the present data show that it is possible to dissociate activations in al or fO using a single subject description, and that in fact performance monitoring recruits fO. Discussion of performance monitoring related activity within this region should therefore be oriented in the light of the anatomo-functional organization of fO, not of al. Further studies using precise protocols to disentangle specific dimensions of performance monitoring will gain important information by using single subject analyses.

## Acknowledgments

This work was supported by the Neurodis Foundation and the French National Research Agency and by the European Research Council under the European Community's Seventh Framework Program (FP7/2007-2013 Grant Agreement n. 241077) grant. This work was performed within the framework of the LABEX CORTEX (ANR-11-LABX-0042) of Université de Lyon, within the program "Investissements d'Avenir" (ANR-11-IDEX-0007) operated by the French National Research Agency (ANR). We thank Dr. Christian Scheiber for the medical monitoring of the subjects in studies 1 and 2. Experimental part of this study was performed at CERMEP–Imagerie du vivant, Bron, F-69677, France, imaging facilities, and at the Marseille fMRI center, F-13005 Marseille, France.

## Author contributions

C.A., E.P., M.W., and B.B. designed research; C.A. and M.W. performed research; C.A. and M.W. analyzed data; C.A., E.P., M.W., B.B., I.F., and M.P. wrote the paper.

## References

- Allman JM, Tetreault NA, Hakeem AY, Manaye KF, Semendeferi K, Erwin JM, Park S, Goubert V, Hof PR (2011) The von Economo neurons in the frontoinsular and anterior cingulate cortex. *Ann N Y Acad Sci* 1225:59-71.
- Amiez C, Kostopoulos P, Champod AS, Petrides M (2006) Local morphology predicts functional organization of the dorsal premotor region in the human brain. *The Journal of neuroscience* 26:2724-2731.
- Amiez C, Petrides M (2007) Selective involvement of the mid-dorsolateral prefrontal cortex in the coding of the serial order of visual stimuli in working memory. *Proc Natl Acad Sci U S A* 104:13786-13791.
- Amiez C, Petrides M (2009) Anatomical organization of the eye fields in the human and non-human primate frontal cortex. *Prog Neurobiol* 89:220-230.
- Amiez C, Hadj-Bouziane F, Petrides M (2012a) Response selection versus feedback analysis in conditional visuo-motor learning. *Neuroimage* 59:3723-3735.
- Amiez C, Sallet J, Procyk E, Petrides M (2012b) Modulation of feedback related activity in the rostral anterior cingulate cortex during trial and error exploration. *Neuroimage* 63:1078-1090.
- Amiez C, Neveu R, Warrot D, Petrides M, Knoblauch K, Procyk E (2013) The location of feedback-related activity in the midcingulate cortex is predicted by local morphology. *The Journal of neuroscience* 33:2217-2228.
- Amiez C, Petrides M (2014) Neuroimaging evidence of the anatomo-functional organization of the human cingulate motor areas. *Cerebral cortex* 24:563-578.
- Amunts K, Schleicher A, Burgel U, Mohlberg H, Uylings HB, Zilles K (1999) Broca's region revisited: cytoarchitecture and intersubject variability. *J Comp Neurol* 412:319-341.
- Amunts K, Lenzen M, Friederici AD, Schleicher A, Morosan P, Palomero-Gallagher N, Zilles K (2010) Broca's region: novel organizational principles and multiple receptor mapping. *PLoS Biol* 8.
- Anwander A, Tittgemeyer M, von Cramon DY, Friederici AD, Knosche TR (2007) Connectivity-Based Parcellation of Broca's Area. *Cerebral cortex* 17:816-825.

- Auzias G, Colliot O, Glaunès JA, Baillet S (2011) Diffeomorphic brain registration under exhaustive sulcal constraints. *IEEE Transactions on Medical Imaging* 30(6):1214 - 1227.
- Becker MP, Nitsch AM, Miltner WHR, Straube T (2014) A single-trial estimation of the feedback-related negativity and its relation to BOLD response in a time-estimation task. *The Journal of neuroscience* 34:3005-3012.
- Brass M, Haggard P (2010) The hidden side of intentional action: the role of the anterior insular cortex. *Brain Struct Funct* 214:603-610.
- Christopoulos GI, Tobler PN, Bossaerts P, Dolan RJ, Schultz W (2009) Neural correlates of value, risk, and risk aversion contributing to decision making under risk. *The Journal of neuroscience* 29:12574-12583.
- d'Acremont M, Lu ZL, Li X, Van der Linden M, Bechara A (2009) Neural correlates of risk prediction error during reinforcement learning in humans. *Neuroimage* 47:1929-1939.
- Damasio H, Frank R (1992) Three-dimensional in vivo mapping of brain lesions in humans. *Arch Neurol* 49:137-143.
- Derrfuss J, Vogt VL, Fiebach CJ, von Cramon DY, Tittgemeyer M (2012) Functional organization of the left inferior precentral sulcus: dissociating the inferior frontal eye field and the inferior frontal junction. *Neuroimage* 59:3829–3837.
- Dosenbach NU, Visscher KM, Palmer ED, Miezin FM, Wenger KK, Kang HC, Burgund ED, Grimes AL, Schlaggar BL, Petersen SE (2006) A core system for the implementation of task sets. *Neuron* 50:799-812.
- Dosenbach NU, Fair DA, Miezin FM, Cohen AL, Wenger KK, Dosenbach RA, Fox MD, Snyder AZ, Vincent JL, Raichle ME, Schlaggar BL, Petersen SE (2007) Distinct brain networks for adaptive and stable task control in humans. *Proc Natl Acad Sci U S A* 104:11073-11078.
- Dutilh, Gilles, Joachim Vandekerckhove, Birte U. Forstmann, Emmanuel Keuleers, Marc Brysbaert, and Eric-Jan Wagenmakers. 2011. "Testing Theories of Post-Error Slowing." *Attention, Perception, & Psychophysics* 74 (2): 454–65. doi:10.3758/s13414-011-0243-2.
- Evrard HC, Logothetis NK, Craig AD (2014) Modular architectonic organization of the insula in the macaque monkey. *J Comp Neurol* 522:64-97.

- Fair DA, Dosenbach NU, Church JA, Cohen AL, Brahmbhatt S, Miezin FM, Barch DM, Raichle ME, Petersen SE, Schlaggar BL (2007) Development of distinct control networks through segregation and integration. *Proc Natl Acad Sci U S A* 104:13507-13512.
- Foundas AL, Weisberg A, Browning CA, Weinberger DR (2001) Morphology of the frontal operculum: a volumetric magnetic resonance imaging study of the pars triangularis. *J Neuroimaging* 11:153-159.
- Friederici AD, Fiebach CJ, Schlesewsky M, Bornkessel ID, von Cramon DY (2006) Processing linguistic complexity and grammaticality in the left frontal cortex. *Cerebral cortex* 16:1709-1717.
- Friston KJ, Penny WD, Glaser DE (2005) Conjunction revisited. *NeuroImage* 25:661-667.
- Friston KJ, Frith CD, Turner R, Frackowiak RS (1995a) Characterizing evoked hemodynamics with fMRI. *Neuroimage* 2:157-165.
- Friston KJ, Frith CD, Frackowiak RS, Turner R (1995b) Characterizing dynamic brain responses with fMRI: a multivariate approach. *Neuroimage* 2:166-172.
- Friston KJ, Holmes AP, Poline JB, Grasby PJ, Williams SC, Frackowiak RS, Turner R (1995c) Analysis of fMRI time-series revisited. *Neuroimage* 2:45-53.
- Harsay HA, Spaan M, Wijnen JG, Ridderinkhof KR (2012) Error awareness and salience processing in the oddball task: shared neural mechanisms. *Front Hum Neurosci* 6:246.
- Higo T, Mars RB, Boorman ED, Buch ER, Rushworth MF (2011) Distributed and causal influence of frontal operculum in task control. *Proc Natl Acad Sci U S A* 108:4230-4235.
- Holroyd CB, Larsen JT, Cohen JD (2004) Context dependence of the event-related brain potential associated with reward and punishment. *Psychophysiology* 41:245-253.
- Keller SS, Roberts N, Hopkins W (2009) A comparative magnetic resonance imaging study of the anatomy, variability, and asymmetry of Broca's area in the human and chimpanzee brain. *The Journal of neuroscience* 29:14607-14616.

- Keller SS, Roberts N, Garcia-Finana M, Mohammadi S, Ringelstein EB, Knecht S, Deppe M (2011) Can the language-dominant hemisphere be predicted by brain anatomy? *Journal of cognitive neuroscience* 23:2013-2029.
- Klein TA, Ullsperger M, Danielmeier C (2013) Error awareness and the insula: links to neurological and psychiatric diseases. *Front Hum Neurosci* 7:14.
- Klein TA, Endrass T, Kathmann N, Neumann J, von Cramon DY, Ullsperger M (2007) Neural correlates of error awareness. *Neuroimage* 34:1774-1781.
- Koban L, Pourtois G (2014) Brain systems underlying the affective and social monitoring of actions: An integrative review. *Neurosci Biobehav Rev. Pt 1*:71-84.
- Menon V, Adleman NE, White CD, Glover GH, Reiss AL (2001) Error-related brain activation during a Go/NoGo response inhibition task. *Hum Brain Mapp* 12:131-143.
- Morel A, Gallay MN, Baechler A, Wyss M, Gallay DS (2013) The human insula: Architectonic organization and postmortem MRI registration. *Neuroscience* 236:117-135.
- Naidich TP, Kang E, Fatterpekar GM, Delman BN, Gultekin SH, Wolfe D, Ortiz O, Yousry I, Weismann M, Yousry TA (2004) The insula: anatomic study and MR imaging display at 1.5 T. *AJNR Am J Neuroradiol* 25:222-232.
- Nelissen N, Stokes M, Nobre AC, Rushworth MF (2013) Frontal and parietal cortical interactions with distributed visual representations during selective attention and action selection. *The Journal of neuroscience* 33:16443-16458.
- Neubert FX, Mars RB, Thomas AG, Sallet J, Rushworth MF (2014) Comparison of human ventral frontal cortex areas for cognitive control and language with areas in monkey frontal cortex. *Neuron* 81:700-713.
- Nieuwenhuys R (2012) The insular cortex: a review. *Prog Brain Res* 195:123-163.
- Nimchinsky EA, Gilissen E, Allman JM, Perl DP, Erwin JM, Hof PR (1999) A neuronal morphologic type unique to humans and great apes. *Proc Natl Acad Sci U S A* 96:5268-5273.
- Oldfield RC (1971) The assessment and analysis of handedness: the Edinburgh inventory. *Neuropsychologia* 9:97-113.

- Petrides M (2014) *Neuroanatomy of Language Regions of the Human Brain*. New York: Academic Press.
- Petrides M, Pandya DN (1994) Comparative cytoarchitectonic analysis of the human and the macaque frontal cortex. In: *Handbook of neuropsychology* (Boller F, Grafman J, eds), pp 17–58. Amsterdam: Elsevier Science.
- Petrides M, Pandya DN (2002) Comparative cytoarchitectonic analysis of the human and the macaque ventrolateral prefrontal cortex and corticocortical connection patterns in the monkey. *Eur J Neurosci* 16:291-310.
- Pizzagalli F, Auzias G, Delon-Martin C, Dojat M. (2013) Local landmark alignment for high-resolution fMRI group studies : Toward a fine cortical investigation of hand movements in human, *Journal of Neuroscience Methods*, 218 (1), 83–95.
- Preuschoff K, Quartz SR, Bossaerts P (2008) Human insula activation reflects risk prediction errors as well as risk. *The Journal of neuroscience* 28:2745-2752.
- Rabbitt, P. M. 1966. "Errors and Error Correction in Choice-Response Tasks." *Journal of Experimental Psychology* 71 (2): 264–72. doi:10.1037/h0022853.
- Ridderinkhof, K. Richard, van den Wildenberg, Wery P. M., Wijnen, Jasper, and Burle, Boris. 2004. "Response Inhibition in Conflict Tasks Is Revealed in Delta Plots." In *Attention*, M. Posner. New York : Guilford Press.
- Rothkirch M, Schmack K, Deserno L, Darmohray D, Sterzer P (2014) Attentional modulation of reward processing in the human brain. *Hum Brain Mapp* 35:3036-3051.
- Rushworth MF, Behrens TE, Rudebeck PH, Walton ME (2007a) Contrasting roles for cingulate and orbitofrontal cortex in decisions and social behaviour. *Trends Cogn Sci* 11:168-176.
- Rushworth MF, Buckley MJ, Behrens TE, Walton ME, Bannerman DM (2007b) Functional organization of the medial frontal cortex. *Curr Opin Neurobiol* 17:220-227.
- Rushworth MF, Noonan MP, Boorman ED, Walton ME, Behrens TE (2011) Frontal cortex and reward-guided learning and decision-making. *Neuron* 70:1054-1069.

- Rutledge RB, Dean M, Caplin A, Glimcher PW (2010) Testing the reward prediction error hypothesis with an axiomatic model. *The Journal of neuroscience* 30:13525-13536.
- Sadaghiani S, D'Esposito M (2014) Functional Characterization of the Cingulo-Opercular Network in the Maintenance of Tonic Alertness. *Cerebral cortex*.
- Seeley WW, Merkle FT, Gaus SE, Craig AD, Allman JM, Hof PR (2012) Distinctive neurons of the anterior cingulate and frontoinsula cortex: a historical perspective. *Cerebral cortex* 22:245-250.
- Seeley WW, Menon V, Schatzberg AF, Keller J, Glover GH, Kenna H, Reiss AL, Greicius MD (2007) Dissociable intrinsic connectivity networks for salience processing and executive control. *The Journal of neuroscience* 27:2349-2356.
- Segal E, Petrides M (2013) Functional activation during reading in relation to the sulci of the angular gyrus region. *Eur J Neurosci* 38:2793-2801.
- Shipp S, Adams RA, and Friston KJ. (2013) Reflections on agranular architecture: predictive coding in the motor cortex. *Trends Neurosci.* 36(12): 706–716.
- Small DM, Zald DH, Jones-Gotman M, Zatorre RJ, Pardo JV, Frey S, Petrides M (1999) Human cortical gustatory areas: a review of functional neuroimaging data. *Neuroreport* 10:7-14.
- Sridharan D, Levitin DJ, Menon V (2008) A critical role for the right fronto-insular cortex in switching between central-executive and default-mode networks. *Proc Natl Acad Sci U S A* 105:12569-12574.
- Tobler PN, Christopoulos GI, O'Doherty JP, Dolan RJ, Schultz W (2009) Risk-dependent reward value signal in human prefrontal cortex. *Proc Natl Acad Sci U S A* 106:7185-7190.
- Tomaiuolo F, Giordano F (2015) Cerebral sulci and gyri are intrinsic landmarks for brain navigation in individual subjects: an instrument to assist neurosurgeons in preserving cognitive function in brain tumour surgery (Commentary on Zlatkina et al.). *Eur J Neurosci.*, doi: 10.1111/ejn.13072.
- Ullsperger M, Harsay HA, Wessel JR, Ridderinkhof KR (2010) Conscious perception of errors and its relation to the anterior insula. *Brain Struct Funct* 214:629-643.

- Vaden KI, Jr., Kuchinsky SE, Cute SL, Ahlstrom JB, Dubno JR, Eckert MA (2013) The cingulo-opercular network provides word-recognition benefit. *The Journal of neuroscience* 33:18979-18986.
- Veldhuizen MG, Douglas D, Aschenbrenner K, Gitelman DR, Small DM (2011) The anterior insular cortex represents breaches of taste identity expectation. *The Journal of neuroscience* 31:14735-14744.
- von Economo CF, Koskinas GN (1925) *Die Cytoarchitektonik der Hirnrinde des Erwachsenen Menschen. Textband und Atlas mit 112 Mikrophotographischen Tafeln.* Wien-Berlin Julius Springer.
- Wessel JR, Danielmeier C, Ullsperger M (2011) Error awareness revisited: accumulation of multimodal evidence from central and autonomic nervous system. *Journal of cognitive neuroscience* 23:3021-3036.
- Yousry TA, Schmid UD, Alkadhi H, Schmidt D, Peraud A, Buettner A, Winkler P (1997) Localization of the motor hand area to a knob on the precentral gyrus. A new landmark. *Brain* 120, 141–157.
- Zlatkina, V., Amiez, C. & Petrides, M. (2015) The postcentral sulcal complex and the transverse postcentral sulcus and their relation to sensorimotor functional organization. *Eur. J. Neurosci.*, doi:10.1111/ejn.13049.

## Table

	Left hemisphere	Right hemisphere
<b>Op8</b>	15	7
<b>Op9</b>	35	44
<b>Op9/cris</b>	45	45
<b>Op8/cris</b>	1	0
<b>al</b>	1	1

**Table 1.** Counts of location of maxima found in individual subjects in each region of interest in the three studies combined.

## Legends

**Fig 1. Anatomical description of the region of interest in a typical subject (S2, study 1), according to Amunts et al. (2010) nomenclature.** Areas 44 and 45 are represented on the cortical surface of the left hemisphere of S2 (left panel). Area 44 is delimited rostrally by the anterior ramus of the lateral fissure (aalf) and caudally by the inferior precentral sulcus (iprs). Area 45 is delimited caudally by the ascending anterior ramus of the lateral fissure (aalf) and rostrally by the horizontal anterior ramus of the lateral fissure (half). Dorsally, both areas 44 and 45 are delimited by the inferior frontal sulcus (ifs). On the left panel, the orange and pink arrows indicate the point of the frontal operculum in the depth of which Op9 and Op8 are located, respectively. Op8 is located adjacent to area 44, at the same anteroposterior level, as it can be observed on the coronal section presented in the bottom right panel (see dotted line on the cortical surface at MNI coordinate Y 12). Op7 is located adjacent to Op8, at the intersection between the operculum and the circular insular sulcus (cris). Op9 is located adjacent to area 45, at the same anteroposterior level, as it can be observed on the coronal section presented in the top right panel (see dotted line on the cortical surface at MNI coordinate Y 21). Op10 is located adjacent to Op9, at the intersection between the operculum and the circular insular sulcus (cris). Note that the limit of Op7 and Op10 within the insular wall is not represented because it has not been described by Amunts et al. (2010). Abbreviations: cs, central sulcus; ds, diagonal sulcus.

**Fig. 2. Protocols. A.** The subjects had to find by trial and error which one of the three stimuli led to the highest juice feedback value (correct feedback) by selecting one stimulus through a press on the corresponding mouse button. Note that the same stimuli appeared on successive trials until the problem was completed, i.e. after discovery and repetition of the correct response. There were four conditions, presented pseudo-randomly, and indicated by the color of the fixation cross throughout the entire trial (see table inset). **B.** The subjects had to find by trial and error which one of the three stimuli led to the correct feedback (i.e. presentation of a green square) by selecting one stimulus through a press on the corresponding mouse button. Note that the same stimuli appeared on successive trials until the problem was completed. **C.** Subjects were instructed to respond with a left or a right button-press to the color of a centrally presented stimulus (e.g. green left, red right).

Concurrently to visual stimulus presentation, an auditory unilateral stimulus was played either compatible or incompatible to the response side. The presence of the distractor led participants to commit errors in 5.6 % of trials.

**Fig 3.** Group analysis: Frontal operculum region involved in the analysis of external juice feedback (15 subjects). **A.** BOLD signal at the occurrence of all juice feedback during exploratory trials (both incorrect and first correct feedback) compared with the BOLD signal at the occurrence of feedback during exploitative trials (i.e. (NEGexplore + POSexplore) minus POSexploit). **B.** Difference in the feedback-related BOLD signal change observed in fO/aI between the negative exploratory and the positive exploitative trials (i.e. NEGexplore minus POSexploit). **C.** Difference in the feedback-related BOLD signal change observed in fO/aI between the first correct exploratory and the positive exploitative trials (i.e. POSexplore minus POSexploit). **D.** Results of conjunction between these two comparisons. Functional maps are represented on sagittal sections in the left (L) and right (R) hemispheres of the average anatomical brain from 15 subjects, at the mediolateral, anteroposterior, and dorsoventral levels described, respectively, by the X, Y, and Z values. The color scale represents the range of t-values. Note that the yellow line represents the location of fO in different anteroposterior levels on coronal slices, in different dorsoventral levels in horizontal slices, and in different mediolateral levels on sagittal slices. Abbreviations: fO, frontal operculum, cris, circular insular sulcus.

**Fig 4.** Group analysis: Frontal operculum region involved in the analysis of external visual feedback (12 subjects). **A.** BOLD signal at the occurrence of all juice feedback during exploratory trials (both incorrect and first correct feedback) compared with the BOLD signal at the occurrence of feedback during exploitative trials (i.e. (NEGexplore + POSexplore) minus POSexploit). **B.** Difference in the feedback-related BOLD signal change observed in fO/aI between the negative exploratory and the positive exploitative trials (i.e. NEGexplore minus POSexploit). **C.** Difference in the feedback-related BOLD signal change observed in fO/aI between the first correct exploratory and the positive exploitative trials (i.e. POSexplore minus POSexploit). **D.** Results of

conjunction between these two comparisons. Functional maps are represented on sagittal sections in the left (L) and right (R) hemispheres of the average anatomical brain from 12 subjects, at the mediolateral, anteroposterior, and dorsoventral levels described, respectively, by the X, Y, and Z values. The color scale represents the range of t-values. Note that the yellow line represents the location of fO in different anteroposterior levels on coronal slices, in different dorsoventral levels in horizontal slices, and in different mediolateral levels on sagittal slices. Abbreviations: fO, frontal operculum, cris, circular insular sulcus.

**Fig 5. Group analysis: Frontal operculum region involved in the analysis of internal (action) feedback (30 subjects).** The BOLD signal at the occurrence of incorrect motor responses is compared to the BOLD signal at the occurrence of correct motor responses. Results are presented on the anatomical average of 30 subjects. They reveal that the maxima of activity is localized bilaterally at the intersection of the frontal operculum and the circular insular sulcus. X, Y, and Z correspond to the X, Y, and Z coordinates within the MNI stereotaxic space. The color scale represents the range of t-values. Note that the yellow line represents the location of fO in different anteroposterior levels on coronal slices, in different dorsoventral levels in horizontal slices, and in different mediolateral levels on sagittal slices. Abbreviations: fO, frontal operculum, cris, circular insular sulcus.

**Fig 6. Conjunction group analysis** between the contrasts (NEGexploire + POSexploire) minus POSexploit) in study 1 (juice feedback) and 2 (visual feedback) and “Error minus Correct” in study 3. Functional maps are represented on sagittal sections in the left (L) and right (R) hemispheres of the average anatomical brain from 45 subjects (15 subjects in Studies 1/2 and 30 subjects in study 3), at the mediolateral, anteroposterior, and dorsoventral levels described, respectively, by the X, Y, and Z values. The color scale represents the range of t-values.

**Fig 7. Subject by subject analysis: Frontal operculum region involved in the analysis of juice external feedback (A), visual external feedback (B), and internal feedback (C)**

in typical subjects. See legends of Figs 3-4. Statistic t-maps thresholded at  $p < 0.001$ , uncorrected.

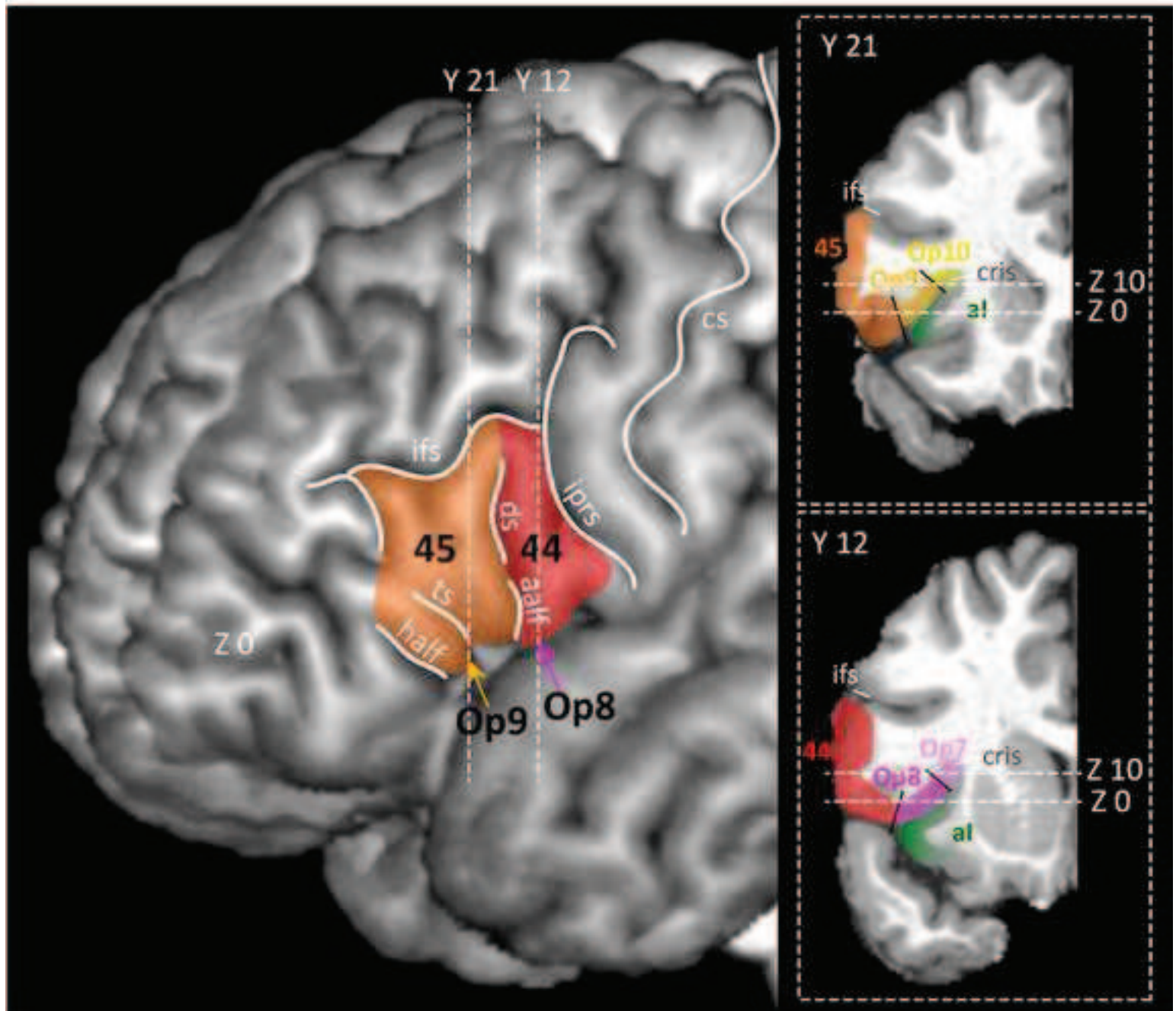
**Fig 8. Distribution of MNI coordinates of increased activity in aI, Op8, Op9, Op8/cris and in Op9/cris observed in individual subjects in Study 1 (A), Study 2 (B), and Study 3 (C).** The figure displays the location of maxima of BOLD signal observed at juice external feedback occurrence in the exploratory period as compared to the exploitative period (A), at visual external feedback occurrence in the exploratory period as compared to the exploitative period (B), and at error trials compared to correct trials (C). Maxima of activity observed in the left and right hemispheres are represented, respectively, as red and blue dots. The radius of the dot represents the size of the t-value of each maximum of activity. Several points can refer to one single subject.

**Fig 9. Relationship between local morphology within the frontal operculum region and activity related to the analysis of juice external feedback (A), visual external feedback (B), and internal feedback (C).** Red and pink circles represent the location of the highest t-value in the frontal operculum, anterior (red) or posterior (pink) to the ascending anterior ramus of the lateral fissure (aalf in fig 1). White circles show the clusters located at the intersection between the frontal operculum (Op9 and Op8) and the circular insular sulcus. Yellow circles represent locations within the insula. Data from all subjects are represented on horizontal sections on the dorso-ventral axis (from MNI coordinates  $Z=9$  to  $Z=-9$ ). Abbreviations: cris: circular insular sulcus, Op9/Op8: frontal Operculum regions, nomenclature following Amunts et al. (2010).

**Fig 10. Extent of activation zone involved in the analysis of juice external feedback (A), visual external feedback (B), and internal feedback (C).** Clusters of activation were extracted in individual subject at a threshold of  $p < 0.001$  (study 1 and 2) or  $p < 0.01$  (study 3) uncorrected, and summed. The resulting color-coded maps show in red an activation zone common to (A) 15 subjects (for the task involving juice external feedback, (B) 12 subjects (for the task involving visual external feedback), and (C) 30 subjects (for the task involving internal feedback) and in purple zones activated only

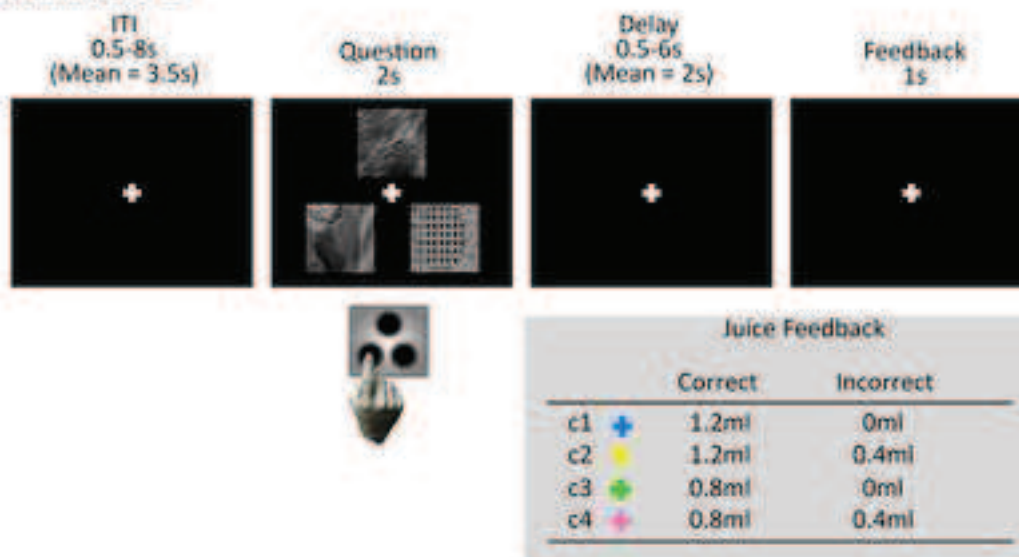
in 1 subject. The figure shows that the region involved in the analysis of juice and visual external feedback and internal feedback is located at the intersection between the circular insular sulcus and fO and spreads into fO. X and Z correspond to the X and Z coordinates within the MNI stereotaxic space. In **(D)** the tractography-based parcellation of the ventrolateral prefrontal region from Neubert et al. (2014) (Reproduced with permission from Neubert et al. 2014) and the superimposition of the 12 subregions resulting from this parcellation onto our anatomical average horizontal sections of interest (at MNI Z coordinates 9, 6, 3, 0, -3, -6, and -9) (with permission to use Supplemental Material “Neuroimaging S2”, Neubert et al. 2014). Data show that the analysis of visual/juice external feedback and internal feedback recruit area 44v and 45 within fO.

FIGURE 1

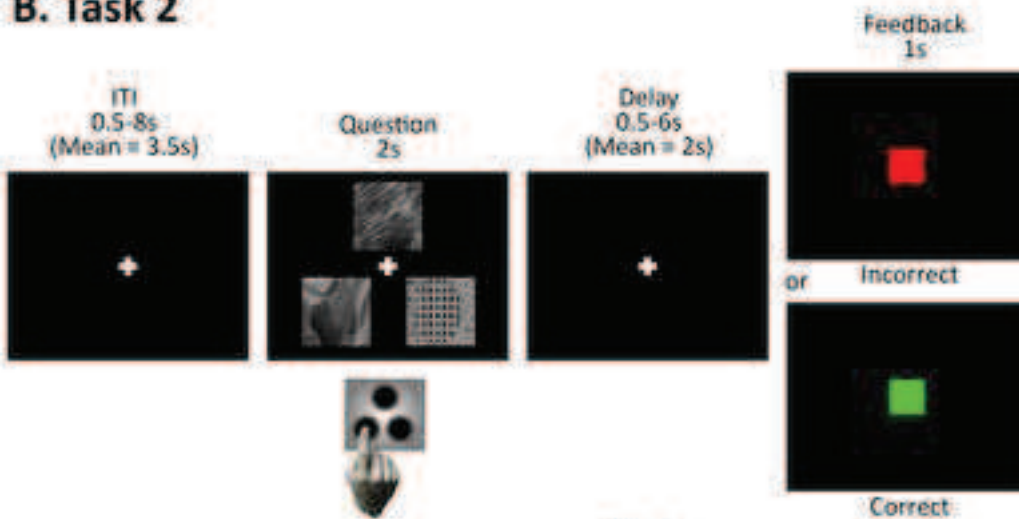


## FIGURE 2

## A. Task 1



## B. Task 2



## C. Task 3

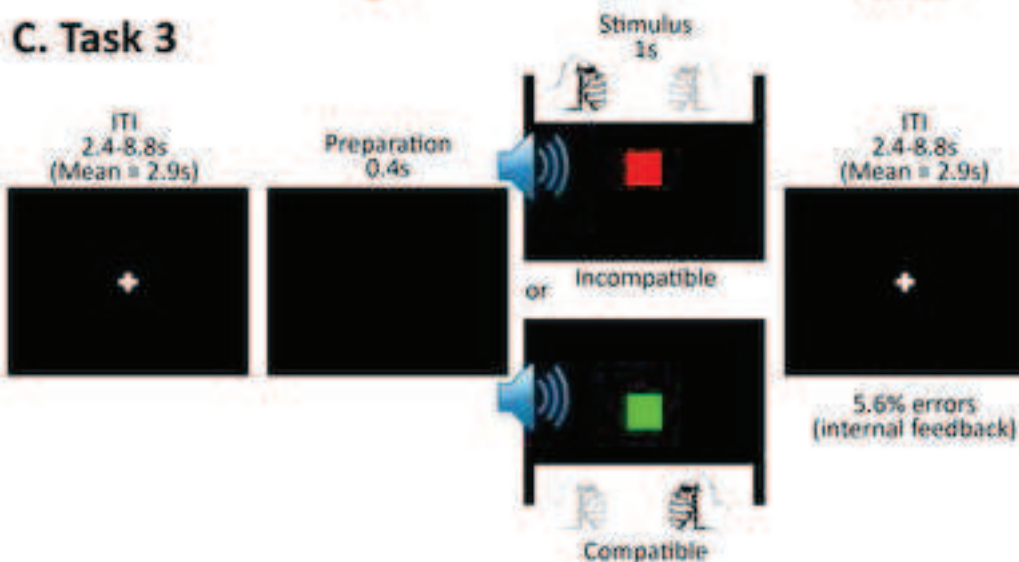


FIGURE 3

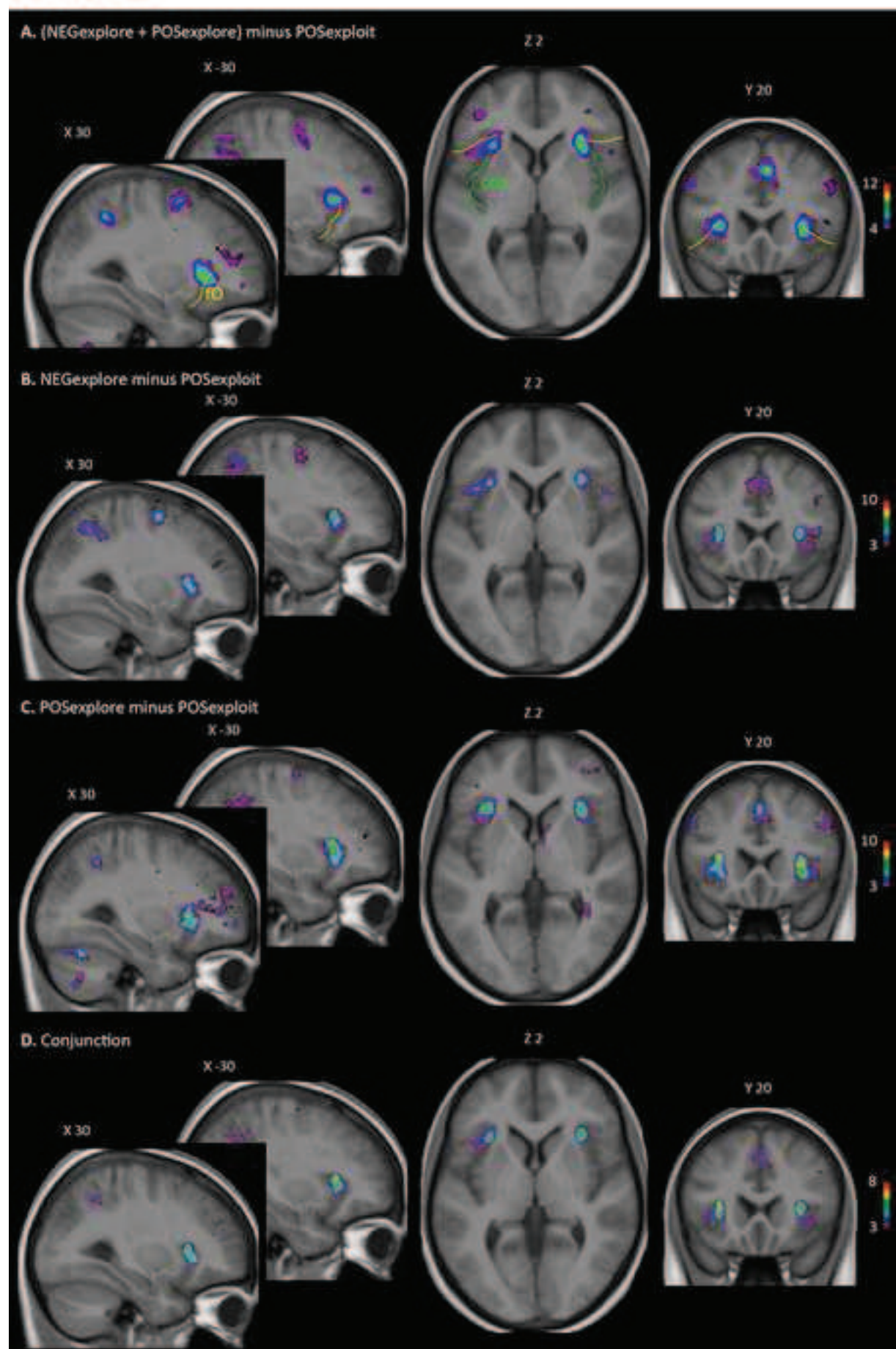


FIGURE 4

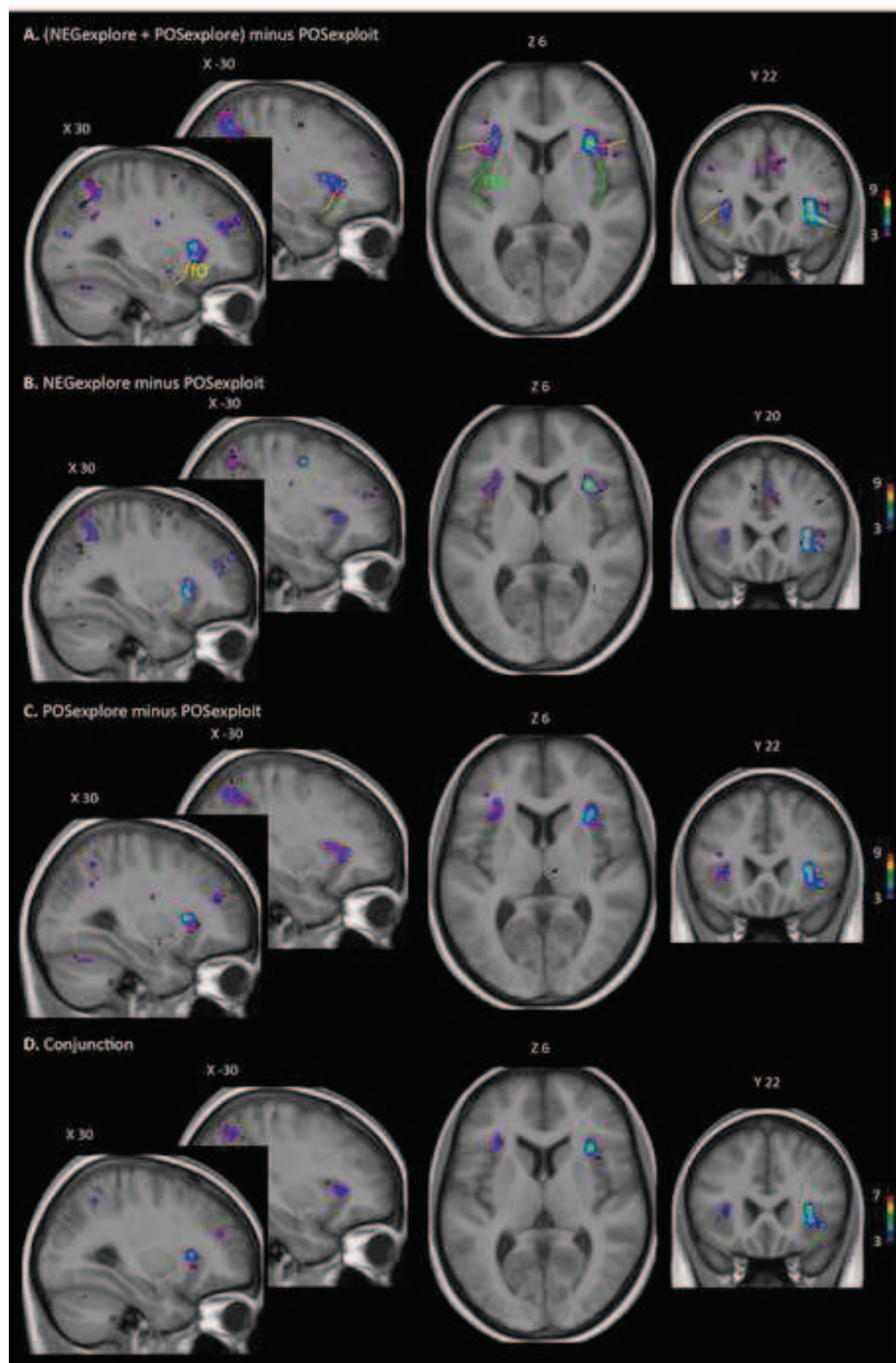
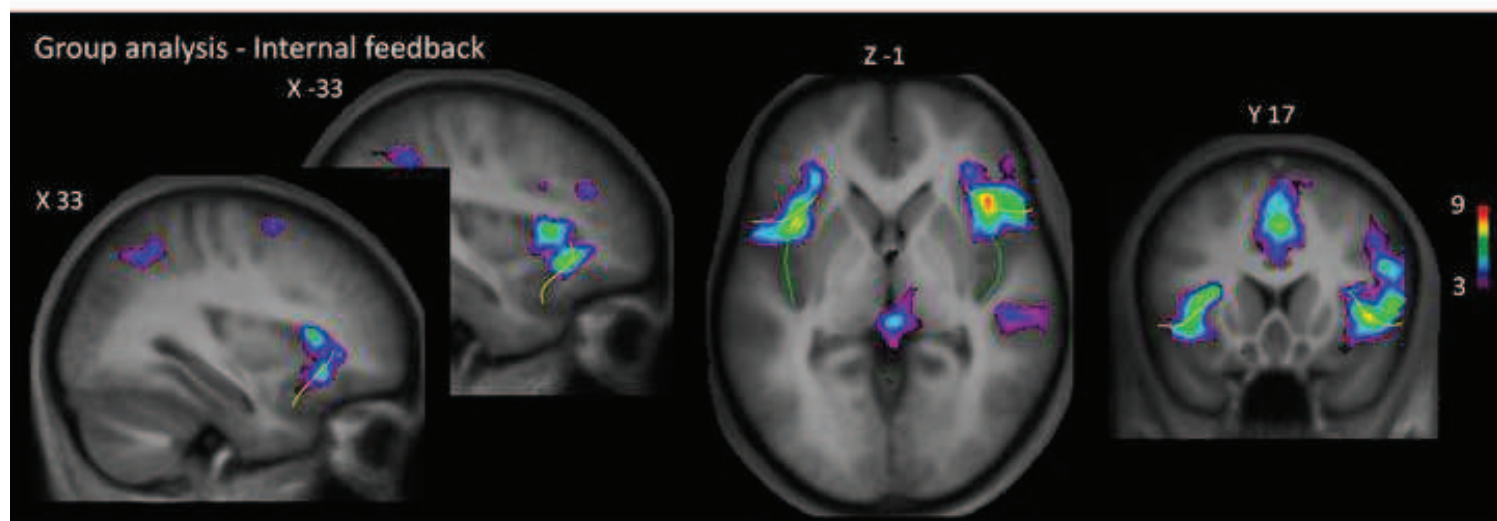
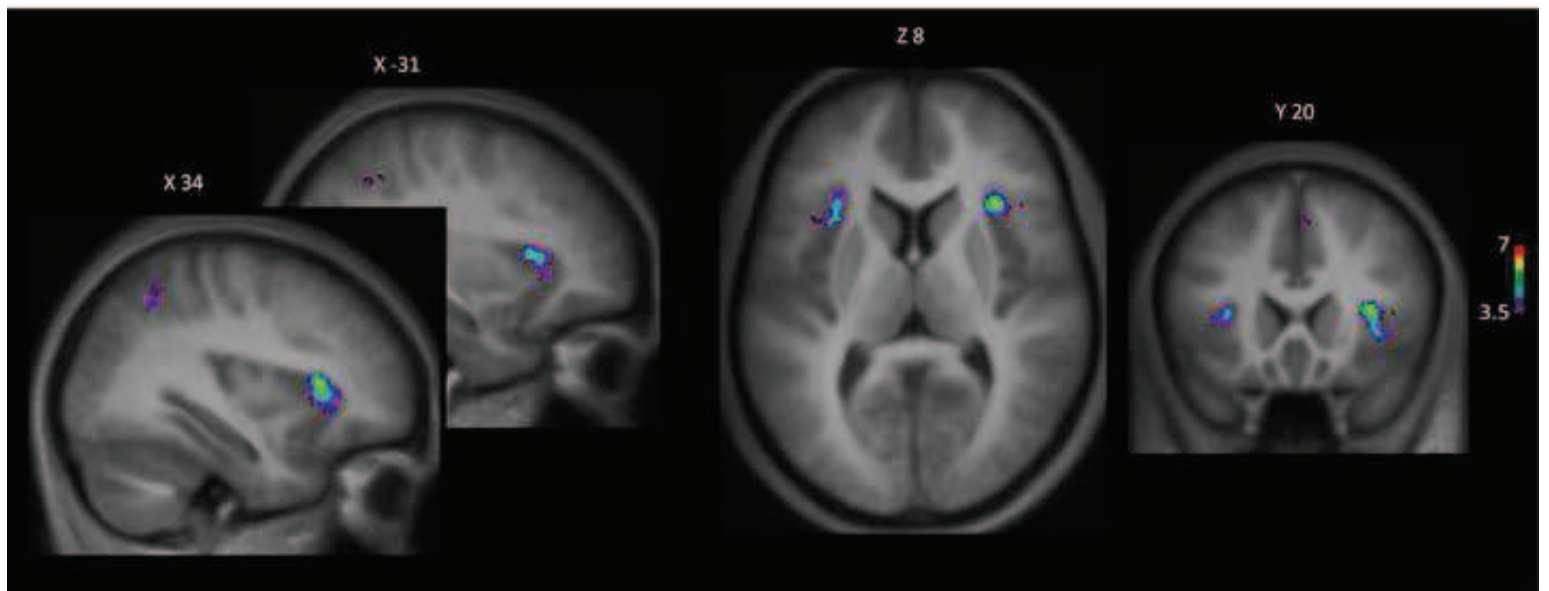


FIGURE 5



SCRIPT

FIGURE 6



AC

## FIGURE 7

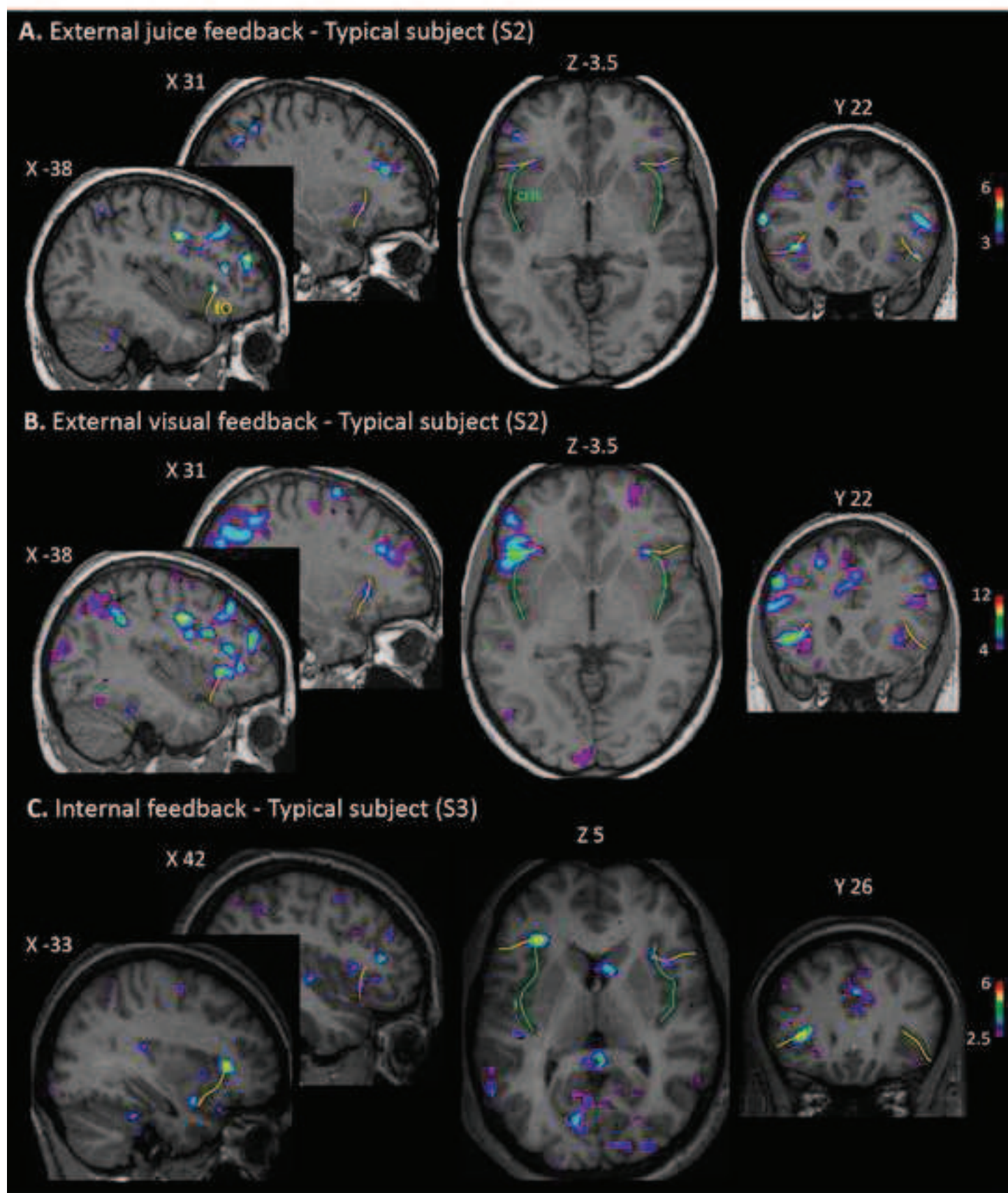


FIGURE 8

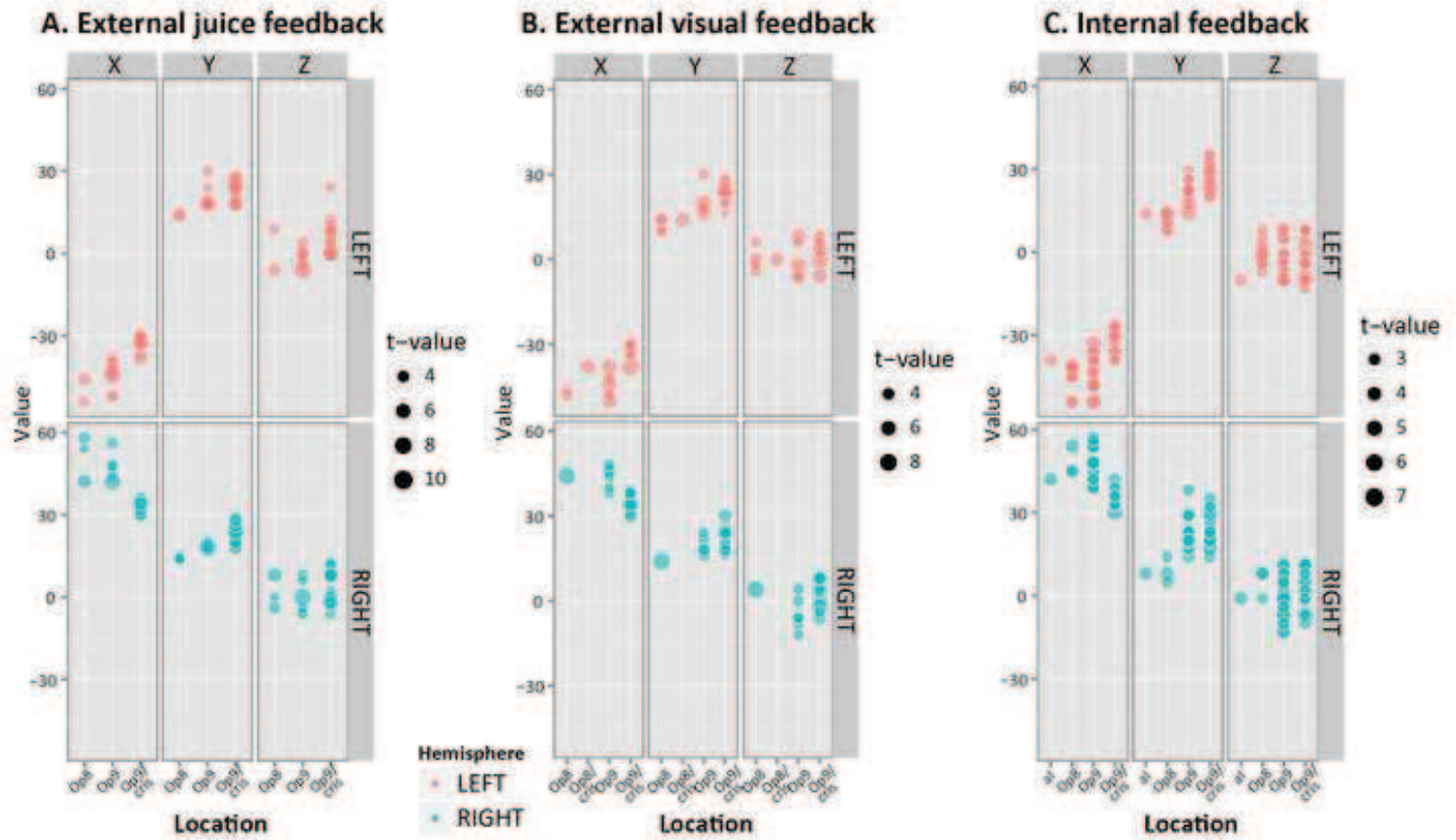


FIGURE 9

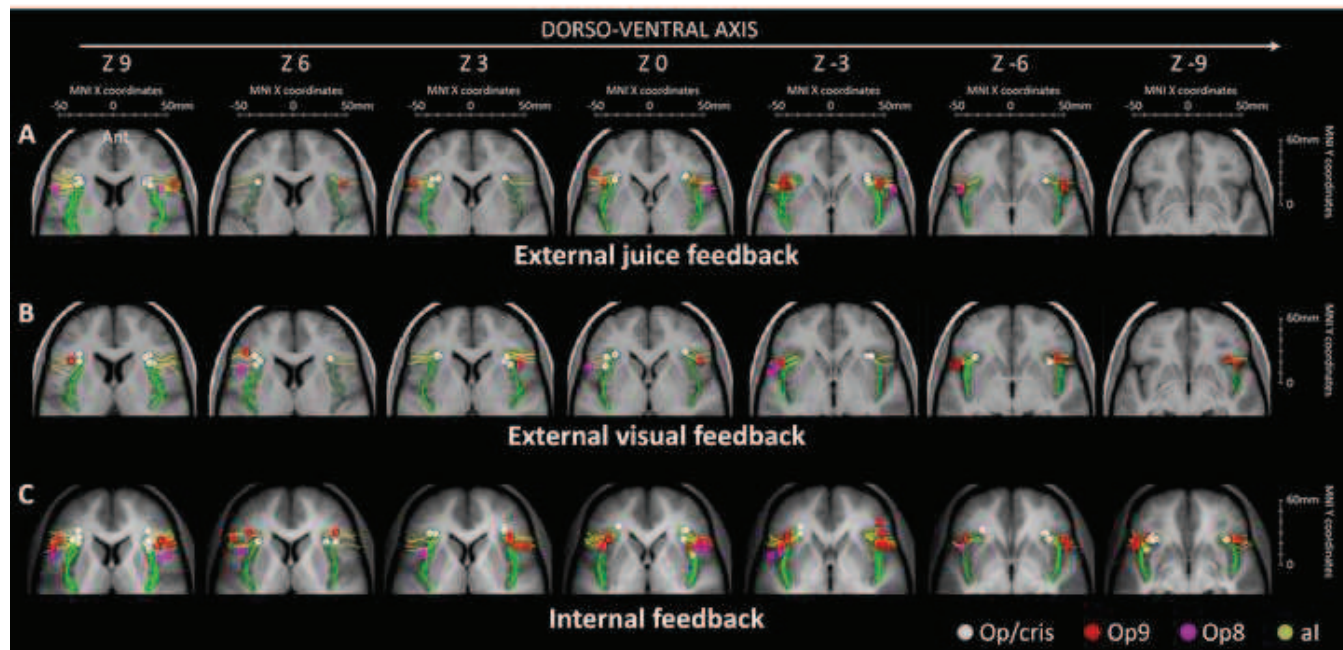
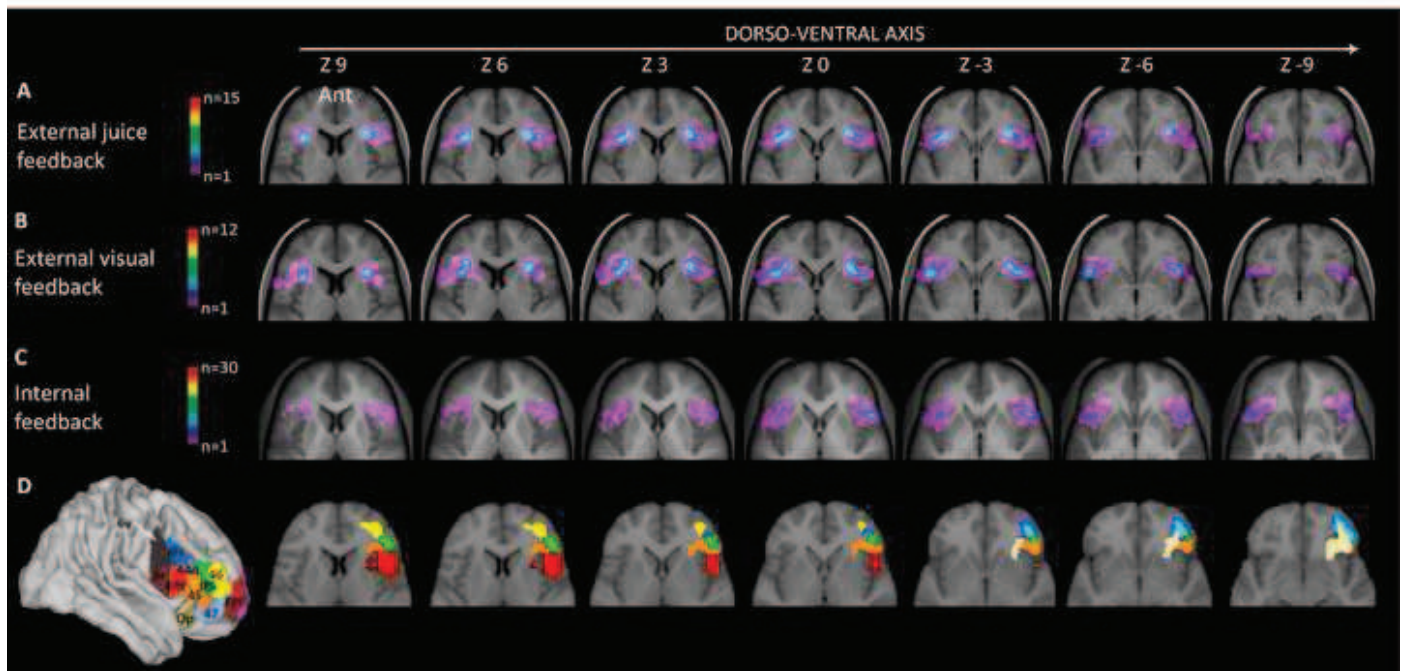


FIGURE 10



## Highlights

- Whether al or fO or both are involved in performance monitoring is debated.
- Relationship between local morphology and activity was assessed on an individual subject basis.
- Results show that performance monitoring-related functional activity is located in fO.
- Local anatomy in this region is a useful tool to disentangle activity issued from al versus fO.